

# Monopoles and dyons in $SO(3)$ gauged Skyrme models

Y. Brihaye<sup>\*</sup>, B. Hartmann<sup>◇</sup> and D. H. Tchrakian<sup>†</sup>

<sup>\*</sup>Physique-Mathematique, Universite de Mons- Hainaut, Mons, Belgium

<sup>◇</sup>Fachbereich Physik, Universität Oldenburg, Postfach 2503, D-26111 Oldenburg, Germany

<sup>†</sup>Department of Mathematical Physics, National University of Ireland Maynooth,  
Maynooth, Ireland

and

School of Theoretical Physics – DIAS, 10 Burlington Road, Dublin 4, Ireland

## Abstract

Three dimensional  $SO(3)$  gauged Skyrme models characterised by specific potentials imposing special asymptotic values on the chiral field are considered. These models are shown to support finite energy solutions with nonvanishing magnetic and electric flux, whose energies are bounded from below by two distinct charges – the magnetic (monopole) charge and a non-integer version of the Baryon charge. Unit magnetic charge solutions are constructed numerically and their properties characterised by the chosen asymptotics and the Skyrme coupling are studied. For a particular value of the chosen asymptotics, charge-2 axially symmetric solutions are also constructed and the attractive nature of the like-monopoles of this system are exhibited. As an indication towards the possible existence of large clumps of monopoles, some consideration is given to axially symmetric monopoles of charges-2,3,4.

# 1 Introduction

In the  $O(4)$ , or usual, Skyrme [1] model in 3 dimensions, the finite energy conditions specify the asymptotic value at large distances of the chiral field uniquely. Depending on the parametrisation, either the  $SU(2)$  valued field  $U$  or the  $S^3$  valued field  $\phi^a$ , subject to  $|\phi^a|^2$ , with  $a = 1, 2, 3, 4$ , this asymptotic value is

$$\lim_{r \rightarrow \infty} U = \mathbb{1} \quad \text{or} \quad \lim_{r \rightarrow \infty} \phi^4 = 1 . \quad (1)$$

The fields  $U$  and  $\phi^a$  are related through

$$U = \phi^a \sigma^a , \quad U^\dagger = \phi^a \tilde{\sigma}^a , \quad (2)$$

where in terms of the Pauli matrices  $\vec{\tau}$ ,  $\sigma^a = (i\tau^i, \mathbb{1})$  and  $\tilde{\sigma}^a = (-i\tau^i, \mathbb{1})$ .

Often, the static Hamiltonian of the Skyrme system is augmented with a 'pion-mass' potential

$$V_\pi(\phi^a) = m_\pi(1 - \phi^4) , \quad (3)$$

consistent with the asymptotics (1). The only practical effect that the inclusion of this potential (3) has is, that it renders the asymptotic behaviour of the chiral function exponential, where in its absence this would have been a power decay.

The situation is very different when the Skyrme model is gauged in one [2] or other [4] gauging prescription, as a result of which the asymptotic value of the chiral field is not fixed uniquely by finite energy conditions. This feature of 3 dimensional gauged Skyrme models was considered and highlighted in [5].

In the present work, we augment the 3 dimensional  $SO(3)$  gauged Skyrme model studied in [3, 4], with the potential<sup>1</sup>

$$V = \lambda(\cos \omega - \phi^4)^2 , \quad \pi \geq \omega \geq 0 , \quad (4)$$

whose effect is to specify the asymptotic values of the chiral field uniquely, consistent with finiteness of the energy. The new asymptotics are

$$\lim_{r \rightarrow 0} \phi^4 = -1 \quad \lim_{r \rightarrow \infty} \phi^4 = \cos \omega . \quad (5)$$

It is clear from (5) that the volume integral of the density that maps the field space to the configuration space, is not going to be an integer except in the case where  $\omega = 0$ . Thus the lower bounds labeled by this charge cannot be identified with the degree of the map, or the topological Baryon charge, except when  $\omega = 0$ . Such a noninteger charge however does supply a legitimate lower bound on the energy integral. For want of a better name, we shall persist in calling such charges  $Q_B(\omega)$ , with the understanding that only  $Q_B(0)$  is really the Baryon charge.

In the generic case  $\pi \geq \omega \geq 0$ , there will be an independent lower bound in addition to  $Q_B(\omega)$ , namely the magnetic monopole flux  $\mu(\omega)$ , which also depends

---

<sup>1</sup>Like (3), this potential is also chosen such that it results in the exponential behaviour of  $\phi^4$  asymptotically.

on  $\omega$ . These lower bounds will be stated explicitly below. The main feature of the dynamics characterised by the potential (4), with  $\omega \neq 0$  is that the  $SO(3)$  is broken down to  $U(1)$ , with the residual Maxwell field described by the corresponding ' Hooft-tensor supporting a magnetic flux. Like the charge  $Q_B(\omega)$ , this magnetic flux  $\mu(\omega)$  is integer also only modulo a continuous factor depending on  $\omega$ , and takes an integer value only when  $\omega = \frac{\pi}{2}$ . The solutions we have found turn out, as expected, to respect both lower bounds  $\mu(\omega)$  and  $Q_B(\omega)$ .

We have confirmed the existence of finite energy solutions bounded by the charges  $\mu(\omega)$  and  $Q_B(\omega)$  by numerical construction. An interesting result is that when  $\omega \neq 0$ , the solution persists even when the Skyrme coupling constant vanishes, i.e.  $\kappa_2 = 0$  in (7) and (8). This is not surprising since the presence of the Yang–Mills term satisfies the (Derrick) scaling requirement independently of the Skyrme term, and in this case, the soliton is bounded from below only by the magnetic flux  $\mu$ . This will be explained in more detail in Section 2, where the model is defined and the two said lower bounds will be stated. Then in Section 3, we study the spherically symmetric solutions for various  $\omega$  and  $\kappa$ , and find the ranges of these two parameters for which solutions exist by numerical construction. In Section 4, we study the axially symmetric magnetic charge-2 solution for the particular value of the parameter  $\omega = \frac{\pi}{2}$ , with a view to learning whether two like monopoles of that system can be in an attractive or a repulsive phase. We encounter the rather surprising result that even for  $\kappa_2 = 0$  this is *attractive*, and then as expected it becomes even more attractive with increasing  $\kappa_2 > 0$ . Section 5 is devoted to summarising and discussing our results.

## 2 The model and lower bounds

The model is specified by the gauging prescription and is the 3 dimensional model used in [3, 4], augmented by the potential (4). Usually, we will treat this potential as a *gedanken* entity and will not exploit it save as an agency justifying the asymptotics (5). In terms of the  $S^3$  valued field  $\phi^a = (\phi^\alpha, \phi^4)$ ,  $\alpha = 1, 2, 3$ , and the  $SO(3)$  gauge connection  $A_\mu^\alpha$  with curvature  $F_{\mu\nu}^\alpha$ , the covariant derivative is defined by the prescription

$$D_\mu \phi^\alpha = \partial_\mu \phi^\alpha + \varepsilon^{\alpha\beta\gamma} A_\mu^\beta \phi^\gamma, \quad D_\mu \phi^4 = \partial_\mu \phi^4. \quad (6)$$

Since much of the analysis will be almost identical to that in (the relevant) Section 3 of [4], we will use the same notation here. This will enable us to present some of the new results without the necessity of repeating the detailed analyses leading to them. The model is described by the Lagrangian

$$\mathcal{L} = -\kappa_0^4 |F_{\mu\nu}^\alpha|^2 + \frac{1}{2} \kappa_1^2 |D_\mu \phi^a|^2 - \frac{1}{2} \kappa_2^4 |D_{[\mu} \phi^a D_{\nu]} \phi^b|^2 - V(\phi^4) \quad (7)$$

which in the temporal gauge  $A_0^\alpha = 0$  yields the static Hamiltonian

$$\mathcal{H} = \kappa_0^4 |F_{ij}^\alpha|^2 + \frac{1}{2} \kappa_1^2 |D_i \phi^a|^2 + \frac{1}{2} \kappa_2^4 |D_{[i} \phi^a D_{j]} \phi^b|^2 + V(\phi^4). \quad (8)$$

The potential  $V(\phi^4)$  in both (7) and (8) is that given by (4). In our study of the 'monopole', we will be mainly concerned with the energy density functional (8), but we give the corresponding Lagrangian (7) too in anticipation of our discussion of the corresponding 'dyon' solution.

We proceed to state the two distinct lower bounds on the energy, namely the volume integral of (8). Both bounds, the 'magnetic monopole' charge and the noninteger 'baryon charge', pertain to the generic asymptotics (5) with  $\omega \neq 0$ , dictated by (4).

The first of these follows from the classic Bogomol'nyi inequality

$$\kappa_0^4 |F_{ij}^\alpha|^2 + \frac{1}{2} \kappa_1^2 |D_i \phi^\alpha|^2 \geq \kappa_0^2 \kappa_1 \varepsilon_{ijk} \partial_k (\phi^\alpha F_{ij}^\alpha) . \quad (9)$$

It is obvious that the left hand side of (9) can be replaced by  $\mathcal{H}$  of (8), by adding suitable positive definite terms to it, resulting in

$$\mathcal{H} \geq \kappa_0^2 \kappa_1 \varepsilon_{ijk} \partial_k (\phi^\alpha F_{ij}^\alpha) , \quad (10)$$

on the right hand side of which we recognise the  $U(1)$  't Hooft-tensor,  $\phi^\alpha F_{ij}^\alpha$ , of the residual gauge field responsible for the magnetic flux provided that  $\omega \neq 0$ , so that  $|\phi^\alpha| \rightarrow \sin \omega \neq 0$  asymptotically.

To state the corresponding inequality for the other lower bound, we define the 'baryon charge' density and its covariantised version, respectively,

$$\varrho_0 = \frac{1}{12\pi^2} \varepsilon_{ijk} \varepsilon^{abcd} \partial_i \phi^a \partial_j \phi^b \partial_k \phi^c \phi^d \quad (11)$$

$$\varrho_G = \frac{1}{12\pi^2} \varepsilon_{ijk} \varepsilon^{abcd} D_i \phi^a D_j \phi^b D_k \phi^c \phi^d . \quad (12)$$

The volume integral of (11) is the noninteger 'baryon charge'

$$\int d^3 x \varrho_0 = (\pi - \omega) N , \quad (13)$$

except when  $\omega = 0$ , when it is simply the integer  $N$ , the degree of the map or the usual baryon charge. The actual gauge invariant charge density which enters the relevant inequality is defined in terms of  $\varrho_G$  in (12) by [3, 4]

$$\varrho = \varrho_G + 3 \varepsilon_{ijk} \phi^\alpha F_{ij}^\alpha D_k \phi^4 , \quad (14)$$

whose volume integral turns out to be equal to the 'baryon charge' (13).

As shown in [4], it follows that

$$\mathcal{H} \geq \frac{\kappa_1 \kappa_2^2}{\sqrt{1 + 9(\frac{\kappa_2}{\kappa_0})^4}} \varrho . \quad (15)$$

We can now conclude from (9) and (15) the two distinct lower bounds on the energy  $E = \int d^3 x \mathcal{H}$ , namely the 'magnetic' and 'baryonic' lower bounds, following

from the asymptotics (5)

$$E \geq 4\pi\kappa_0^2\kappa_1 \sin \omega \quad (16)$$

$$E \geq \frac{12\pi\kappa_1\kappa_2^2}{\sqrt{1 + 9\left(\frac{\kappa_2}{\kappa_0}\right)^4}}(\pi - \omega) . \quad (17)$$

The two inequalities (16) and (17) signal the possibility of finding finite energy solutions bounded from below, provided that the (Derrick) scaling requirement is satisfied, which for (8) in 3 dimensions, it is. For the limiting case of  $\omega = 0$  considered in [4], inequality (16) trivialises and (17) then coincides with the lower bound used in [4]. In the other limit when  $\omega = \pi$ , both (16) and (17) trivialise so we would expect to find no nontrivial solutions in this case. This will be confirmed by our numerical results to be given below. For generic values of  $\omega$  between these two limiting values, both lower bounds are valid independently, and any nontrivial finite energy solution must respect these. This will also be confirmed by our numerical results.

It should perhaps be pointed out that neither of the bounds (10) and (15) can be saturated. As we shall see in Section 3, for  $\omega \neq 0$  finite energy solutions persist also for  $\kappa_2 = 0$ . But even in that case, the inequality (10) cannot be saturated. Thus in the  $\kappa_2 = 0$  model, we have a system which does not saturate a Bogomol'nyi bound and whose stress-energy tensor therefore never vanishes. It follows that the charge-2 monopole of this model is *either* attractive *or* repulsive, a property which it shares with the usual (ungauged) Skyrme model [1], in the latter case as is well known it being attractive [6]. We shall find in Section 4 that the model with  $\kappa_2 = 0$  supports solutions describing mutually attracting like monopoles. Then as expected, when the Skyrme coupling constant  $\kappa_2$  is switched on this binding energy will grow further as is usual with other theories [7] involving Skyrme like kinetic terms.

### 3 Spherically symmetric solutions

This Section is divided into two Subsections, in the first of which we present the reduced one dimensional subsystems of (7) and (8), while in the second we present our numerical results.

#### 3.1 One dimensional subsystems

As in [4], we impose the spherical symmetry thus

$$A_0^\alpha = \kappa_1^{-1}g(r) \hat{x}^\alpha , \quad A_i^\alpha = \frac{a(r) - 1}{r} \varepsilon_{i\alpha\beta} \hat{x}^\beta , \quad (18)$$

$$\phi^\alpha = \sin f(r) \hat{x}^\alpha , \quad \phi^4 = \cos f(r) . \quad (19)$$

The ensuing reduced one dimensional Lagrange and (static) Hamiltonian, subject to a suitable rescaling  $r \rightarrow x$  such that all constants but the Skyrme coupling  $\kappa_2^4 \equiv \kappa$

are suppressed, are respectively

$$L = -2 \left( 2a'^2 + \frac{(a^2 - 1)^2}{x^2} \right) - \frac{1}{2} (x^2 f'^2 + 2a^2 \sin^2 f) - 2\kappa a^2 \sin^2 f \left( 2f'^2 + \frac{a^2 \sin^2 f}{x^2} \right) + x^2 g'^2 + 2a^2 g^2 \quad (20)$$

$$H = 2 \left( 2a'^2 + \frac{(a^2 - 1)^2}{x^2} \right) + \frac{1}{2} (x^2 f'^2 + 2a^2 \sin^2 f) + 2\kappa a^2 \sin^2 f \left( 2f'^2 + \frac{a^2 \sin^2 f}{x^2} \right) \quad (21)$$

Note that we have suppressed the potential terms arising from (4) in (20) and (21), since as will be explained below, nearly all our numerical constructions will be carried out in the  $\lambda = 0$  limit.

While (21) is positive definite, (20) is not. The latter will be relevant only in some remarks below concerning the dyon solution of this system.

Let us first consider the case of main interest, namely the monopole solutions of the equations following from the static energy density functional (21). The finite energy conditions require the following asymptotic values

$$\lim_{x \rightarrow 0} f(x) = \pi, \quad \lim_{x \rightarrow \infty} f(x) = \omega \quad (22)$$

$$\lim_{x \rightarrow 0} a(x) = 1, \quad \lim_{x \rightarrow \infty} a(x) = 0, \quad (23)$$

as long as  $\omega \neq 0$ . This is the case of interest in the present work. (The  $\omega = 0$ , which is only a limiting case here, was studied in detail in [4].)

The behaviours of the functions  $f(x)$  and  $a(x)$  in the  $x \ll 1$  region are independent of the value of  $\lambda$  in (4), and they are

$$f(x) = \pi + F_1 x + o(x^3), \quad (x \ll 1) \quad (24)$$

$$a(x) = 1 + A_1 x^2 + o(x^4), \quad (x \ll 1) \quad (25)$$

In the  $x \gg 1$  region, the asymptotic behaviour of the function  $a(x)$  is again independent of the value of  $\lambda$  and is

$$a(x) = A e^{-\frac{1}{2}x \sin \omega}, \quad A = \text{const.}, \quad (26)$$

while that of the function  $f(x)$  does depend on  $\lambda$ . In the limit of vanishing  $\lambda$  and finite  $\lambda$ , these are respectively the power and exponential decays

$$f(x) = \omega + \frac{F}{x} + o\left(\frac{1}{x^2}\right), \quad (27)$$

$$f(x) = \omega + \tilde{F} \frac{e^{-\sqrt{2\lambda}x}}{x}, \quad (28)$$

where  $F$  and  $\tilde{F}$  are constants which can be evaluated by the numerical process.

Thus, like with the usual (ungauged) Skyrme model, the addition of this potential results in the exponential localisation of the chiral function  $f(r)$ . In the numerical

work presented in the next two Subsections we have used  $\lambda = 0$  throughout, since the qualitative properties of the solutions are unchanged when  $\lambda > 0$ . This was verified in many typical cases and thereafter the potential (4) played a *Gedanken* rôle, rather like for the Prasad–Sommerfield limit of the Georgi–Glashow model, except that here the  $\lambda = 0$  limit is not particularly interesting since it does not lead to the saturation of any Bogomol’nyi bound.

### 3.1.1 Dyon solution

Before proceeding to describe our numerical results concerning the monopole solutions of this model, we briefly allude to the corresponding dyon solutions. Following Julia and Zee [8] we vary the energy density (20) with respect to the functions  $a(r)$ ,  $g(r)$  and  $f(r)$ . Since (20) is not positive definite, the radial Ansatz (18) and (19) is not guaranteed to be consistent with the full Euler–Lagrange equations of this system. It has however been verified in [9] that (18)–(19) is indeed consistent.

The crucial equation that signals the existence of a dyon solution is the  $r \gg 1$  asymptotic equation arising from the variation of the function  $a(x)$

$$a'' = a \left( \frac{a^2 - 1}{x^2} - g^2 + \sin^2 f + \dots \right) \quad (29)$$

which in the  $x \rightarrow \infty$  limit reduces to

$$a'' = (\sin^2 \omega - g^2)a ,$$

which yields acceptable exponentially decaying solutions only when the asymptotic value of  $q = \lim_{x \rightarrow \infty} g(x)$  satisfies the condition

$$0 \leq q \leq \sin \omega , \quad (30)$$

and otherwise leading to unacceptable oscillatory behaviour for the function  $a(r)$  asymptotically.

With the asymptotic condition (30), one has the behaviour

$$g(x) = q - \frac{c}{x} + o(x^{-2}) , \quad (31)$$

in which the constant  $c$  is evaluated by the numerical integrations and parametrises the electric flux of the dyon. We do not repeat here the detailed results of the numerical process as this is identical to that for the dyon [8] of the Georgi–Glashow model, as presented in [9]. The relevant analysis in Section V of Ref.[9] can be adapted to the present model, by substituting the condition  $0 \leq q \leq 1$  there, by (30).

The only qualitative difference between the dyon of the Georgi–Glashow model and the dyon of the present model is, that unlike in the former case here there is no Prasad–Sommerfield limit.

### 3.2 Numerical results

Solving the spherically symmetric equations for numerous values of the parameters  $\kappa \in ]0, \infty[$  and  $\omega \in ]0, \pi[$ , strongly indicates that they admit at least one regular, finite-energy solution for each choice of these parameters.

The behaviour of the solution in the limit  $\omega \rightarrow 0$  is different according to the value of  $\kappa$  and is strongly influenced by the pattern of solutions occurring in the case  $\omega = 0$ . We briefly recall (see [4, 9] for further details) that for  $\omega = 0$ , solutions with  $a(\infty) = 0$  exist only for  $\kappa > \kappa_{cr}$ ,  $\kappa_{cr} \approx 0.697$ . For  $\kappa \in ]0, 0.697[$  the relevant solution has  $a(\infty) = 1$ .

Let us now describe how the solutions look like for fixed  $\kappa$ , with  $\omega$  varying. We have found it convenient to characterise the solutions by the value of the asymptotic coefficient  $F$  defined in Eq. (27). The evolution of this parameter is reported in Fig. 1 for several values of  $\kappa$ . For  $\kappa > \kappa_{cr}$  the solutions are such that the function  $f(x)$  (resp.  $a(x)$ ) decreases monotonically from  $\pi$  (resp. 1) for  $x = 0$  to  $\omega$  (resp. 0) for  $x \rightarrow \infty$ . The parameter  $F$  is positive as seen in Fig. 1 for  $\kappa = 1.0$ . The classical energy decreases monotonically when  $\omega$  increases. In the limit  $\omega \rightarrow 0$  the classical solution of [4] are smoothly approached.

The behaviour of the solutions is more elaborate when  $\kappa < \kappa_{cr}$ ; this is illustrated on Fig. 1 and on Fig. 2 for  $\kappa = 0.1$ . One new feature is that the parameter  $F$  undergoes a change of sign when  $\omega$  varies from 0 to  $\pi$ . For large enough values of  $\omega$  (say,  $\omega > \omega_{max}$ ,  $\omega_{max} \approx 0.5$  in the case  $\kappa = 0.1$ ), the profiles of  $f(x)$  and of  $a(x)$  monotonically decrease as functions of  $x$  and the classical energy decreases for  $\omega$  increasing. For  $\omega < \omega_{max}$  the function  $f(x)$  develops a local minimum at an intermediate value of  $x$  and the parameter  $F$  defined in Eq.(27) becomes negative. Moreover, the function  $a(x)$  develops a local minimum and a local maximum at finite values (say  $x_m, x_M$ ) of the radial variable. In this region of  $\omega$  the classical energy increases with  $\omega$ . When the limit  $\omega \rightarrow 0$  is considered our numerical analysis indicates that  $x_m$  stays finite,  $x_M$  increases and the value  $a(x_M)$  approaches  $a = 1$  in such a way that the corresponding profile of the  $\omega = 0$  solution is approached on  $[0, x_M]$ . The corresponding value of the classical energy is also reproduced. These different features are illustrated on Figs. 1,2.

Considered as a function of  $\omega$ , we also observed (see Fig. 2) that the classical energy is maximal at an intermediate value of  $\omega$ . Our numerical analysis indicates that the maximum is attained precisely for  $\omega = \omega_{max}$ , i.e. at the value where the change of sign of the parameter  $F$  occurs. The  $\kappa$ -dependence of  $\omega_{max}$  is reported on Fig. 3.

As further suggested by Fig. 1, in the region  $\kappa \approx 0.5$ ,  $\omega \approx 0.05$  the pattern of the solutions becomes very complicated. We obtained strong numerical evidence that several branches of solutions exist in this region. That is to say e.g, that we find more than one solution for  $\kappa = 0.5$ ,  $\omega = 0.05$ . However these new branches seem to exist on a very small domain of the parameter  $\omega$ , the numerical analysis is therefore rather difficult in this region. Since the study of such details is not the aim of the present paper, we refrained from further pursuing our numerical analysis in this region.

To finish this section, we mention that, choosing  $\kappa = 0$ , we were able to construct numerical solutions for  $\omega > 1.1729$ . The analysis of the solutions in the limit  $\kappa \rightarrow 0$  (with fixed  $\omega < 1.1729$ ), seems to lead to a discontinuity of the function  $f(x)$ .

## 4 Axially symmetric solutions

This Section is divided in two Subsections as in the previous Section, in the first of which the axially symmetric Ansatz, and, the boundary conditions of the axially symmetric solutions, are stated. In the second Subsection, the numerical results are given.

Our objective in this Section is to construct higher magnetic charge solutions, and in the first instance charge-2 axially symmetric solutions, with the aim of discovering whether like monopoles of this model are in an attractive or a repulsive phase. In this framework, we will restrict our analysis to monopole rather than dyon solutions, in the temporal gauge  $A_0 = 0$ .

The analysis carried out in this Section is less general than that given in the previous Section for the spherically symmetric solutions. There, we studied the detailed dependence of the solutions on the parameter  $\omega$  specifying the dynamics. Having exposed these properties satisfactorily, we proceed to study the most natural subset of models here, namely those specified by  $\omega = \frac{\pi}{2}$ , supporting monopoles of *integer* magnetic charges.

Within this  $\omega = \frac{\pi}{2}$  subset of models, we consider the models specified by the Skyrme coupling  $\kappa_2$ , or, the effective parameter  $\kappa$  for the range  $\kappa \geq 0$  which includes interestingly the point  $\kappa = 0$ .

### 4.1 Ansatz and boundary conditions

With magnetic charge, or azimuthal winding,  $n = 1, 2, 3, \dots$ , the axially symmetric Ansatz [10] for the gauge field is

$$A_\mu dx^\mu = \frac{1}{2r} \left[ \tau_\phi^n (H_1 dr + (1 - H_2) r d\theta) - n (\tau_r^n H_3 + \tau_\theta^n (1 - H_4)) r \sin \theta d\phi \right], \quad (32)$$

and for the Skyrme field it is

$$U = \frac{1}{2} (\cos f \mathbb{1} + \sin f [(\sin g \sin \theta + \cos g \cos \theta) \tau_r^n + (\sin g \cos \theta - \cos g \sin \theta) \tau_\theta^n]) . \quad (33)$$

where  $H_1, H_2, H_3, H_4, f$  and  $g$  are functions of the coordinates  $r$  and  $\theta$ . The symbols  $\tau_r^n, \tau_\theta^n$  and  $\tau_\phi^n$  denote the dot products of the cartesian vector of Pauli matrices,  $\vec{\tau} = (\tau_x, \tau_y, \tau_z)$ , with the spatial unit vectors

$$\begin{aligned} \vec{e}_r^n &= (\sin \theta \cos n\phi, \sin \theta \sin n\phi, \cos \theta) , \\ \vec{e}_\theta^n &= (\cos \theta \cos n\phi, \cos \theta \sin n\phi, -\sin \theta) , \\ \vec{e}_\phi^n &= (-\sin n\phi, \cos n\phi, 0) , \end{aligned} \quad (34)$$

respectively.

For  $n = 1$ ,  $H_1 = H_3 = 0$ ,  $H_2 = H_4 = a(r)$ ,  $f = f(r)$  and  $g = \theta$  the spherically symmetric ansatz of (18)-(19) is recovered.

The residual  $U(1)$  gauge degree of freedom [10] is fixed by the condition  $r\partial_r H_1 - \partial_\theta H_2 = 0$ , which is just the Coulomb gauge in the two dimensional residual  $U(1)$  subsystem resulting from the imposition of radial symmetry in the  $x - y$  plane, i.e. with radius  $\rho = \sqrt{x^2 + y^2}$ .

At the origin the boundary conditions for the gauge field functions read

$$H_2|_{r=0} = H_4|_{r=0} = 1, \quad H_1|_{r=0} = H_3|_{r=0} = 0, \quad (35)$$

and for the Skyrme functions

$$f|_{r=0} = \pi, \quad \partial_r g|_{r=0} = 0. \quad (36)$$

For the gauge field to approach the asymptotic configuration of a monopole we choose

$$H_2|_{r=\infty} = H_4|_{r=\infty} = 0, \quad H_1|_{r=\infty} = H_3|_{r=\infty} = 0, \quad (37)$$

and for the Skyrme field functions

$$f|_{r=\infty} = \omega, \quad g|_{r=\infty} = \theta. \quad (38)$$

The boundary conditions along the  $\rho$ - and  $z$ -axis are determined by the symmetries. For the gauge field functions symmetry considerations lead to the boundary conditions

$$\begin{aligned} H_1|_{\theta=0} &= H_3|_{\theta=0} = 0, & \partial_\theta H_2|_{\theta=0} &= \partial_\theta H_4|_{\theta=0} = 0, \\ H_1|_{\theta=\pi/2} &= H_3|_{\theta=\pi/2} = 0, & \partial_\theta H_2|_{\theta=\pi/2} &= \partial_\theta H_4|_{\theta=\pi/2} = 0 \end{aligned} \quad (39)$$

along the axes, as well as the condition

$$H_2|_{\theta=0} = H_4|_{\theta=0}. \quad (40)$$

Along these axes the Skyrme field functions satisfy the following boundary conditions;

$$\begin{aligned} \partial_\theta f|_{\theta=0} &= 0, & \partial_\theta g|_{\theta=0} &= 1, \\ \partial_\theta f|_{\theta=\pi/2} &= 0, & \partial_\theta g|_{\theta=\pi/2} &= 1 \end{aligned} \quad (41)$$

## 4.2 Numerical results

Solving the set of partial differential equations numerically for the model characterised by  $\omega = \pi/2$ , and for different values of  $\kappa$ , we find that even for  $\kappa = 0$  there is only an attractive phase. As shown in Fig. 4, the difference  $\delta E$  of the energy per winding number  $n$  between the  $n = 1$  and  $n = 2$  increases with increasing  $\kappa$ . This is an indication that in this model 2-monopole bound states can exist. Although a definitive demonstration of this is well beyond the scope of the present work. (That

would involve finding the dependence of the interaction energy on the separation of the two monopoles.)

Moreover, we calculated the energy  $E_n(\kappa)$ , for different values of  $\kappa$  and  $n$ . The values are given in the tables below. Unfortunately the numerical process becomes less reliable with increasing monopole charge  $n$ . As a result we restrict our numerical constructions to  $n \leq 4$  only. For  $\kappa = 0$ ,  $\kappa = 3$  and  $\kappa = 5$  we find

$n$	1	2	3	4
$E_n(0)$	2.95	4.82	6.63	7.56

$n$	1	2	3	4
$E_n(3)$	3.40	5.40	7.30	8.80

$n$	1	2	3	4
$E_n(5)$	3.48	5.60	7.50	9.31

From this data we can deduce some quantitative information on the interaction energies of the monopoles leading to the possible formation of lumps of charges  $n \leq 4$ . To this end we define the following 'binding energy' corresponding to the energy needed to dissociate a charge- $n$  lump into a charge- $n-1$  and a charge-1 lump, divided by the energy of the charge- $n$  lump.

$$\Delta E_n^{\{n-1,1\}}(\kappa) = \frac{[E_{n-1}(\kappa) + E_1(\kappa)] - E_n(\kappa)}{E_n(\kappa)}. \quad (42)$$

The values for different  $\kappa$  and  $n$  are given in the Table below.

$n$	$\Delta E_n^{\{n-1,1\}}(0)$	$\Delta E_n^{\{n-1,1\}}(3)$	$\Delta E_n^{\{n-1,1\}}(5)$
2	0.22	0.26	0.24
3	0.17	0.21	0.21
4	0.27	0.22	0.18

This table shows that for all three values of  $\kappa$ ,  $\Delta E_n^{\{n-1,1\}}(\kappa)$  remains positive, which is an indication for the existence of monopole lumps of charges up to  $n = 4$ .

It is hard to extract any reliable conclusion from such meagre data, but the fact that the binding energies do not seem to decrease with increasing  $n$  is encouraging from the point of view of the possibility of finding very large monopole clumps. This question will be investigated elsewhere, using different numerical techniques.

## 5 Summary and Discussion

We have studied a particular variant of the Skyrme model gauged according to the prescription (6), equivalent to the commutator gauging with respect to the  $SU(2)$  gauge connection  $A_i = -\frac{i}{2}\vec{A}_i \cdot \vec{\tau}$ ,

$$D_i U = \partial_i U + [A_i, U], \quad (43)$$

which is augmented by the potential (4). The function of this potential is to fix the boundary value of the Skyrme field at large distances which, unlike in the usual (ungauged) Skyrme model, is not fixed by the requirement of finite energy<sup>2</sup>. Thus we have considered a set of the gauged Skyrme models characterised by the parameter  $\omega$  appearing in the potential (4). In the usual Skyrme model  $\omega = 0$ .

The qualitative properties of the solitons, depending on the parameters  $\omega$  and  $\kappa$  characterising the models, are studied in the spherically symmetric case.

The main effect of the boundary condition  $\omega \neq 0$  is the breaking of the  $SO(3)$  gauge symmetry of the solution down to  $SO(2)$ , asymptotically. This is related to the nonvanishing VEV of the Skyrme field  $\phi^\alpha$ . This can be seen clearly from the second member of (5). In addition to this magnetic charge, a noninteger version of the Baryon number given by (13) is also associated with this solution. We have verified the existence of finite energy solutions bounded from below by both these charges for the allowed ranges of  $\omega$ . The latter (ranges) depend also on the (effective) Skyrme coupling  $\kappa$  of the model. These ranges have been illustrated in Fig. 1.

A surprising if not unexpected property of these models is, that the model characterised by  $\kappa = 0$  does support a soliton. This could have been expected since in the presence of the Yang–Mills term, it is not necessary to have a Skyrme term to satisfy the (Derrick) scaling requirement. We found that the solitons of the  $\kappa = 0$  models are generally quite similar to those of the the models with  $\kappa \neq 0$ , with one noticeable qualitative difference. This concerns the restricted range of allowed  $\omega$  for the  $\kappa = 0$  model as seen in Fig. 1, (and in Fig. 3) which in addition to this qualitative feature also illustrates the fact that for small enough  $\kappa$  the profile of the chiral function  $f(r)$  sinks below its asymptote  $\omega$  and approaches it from below.

By contrast when  $\omega = 0$ , the model with  $\kappa = 0$  cannot support a soliton because in that case the lower bound (10) disappears, leaving only the lower bound (13) in place, and the latter trivialises in the  $\kappa = 0$  limit. This is also borne out by the graphs in Fig. 1.

After exposing the qualitative features of the solitons in the spherically symmetric case, we studied axially symmetric solutions of the model. Our aim here was to discover if like monopoles of the  $\omega \neq 0$  models are in attractive or repulsive phases. For this purpose we restricted ourselves to the  $\omega = \frac{\pi}{2}$  model which has the nice feature of having integer magnetic charge. We did however consider varying values of the (effective) Skyrme parameter  $\kappa$ , including the distinguished case of  $\kappa = 0$ .

The main interest in the model specified by  $\kappa = 0$  in this respect is that, like the usual (ungauged) Skyrme model, it exhibits no free coupling constants that can parametrise the crossover from an attractive to a repulsive phase. Like the latter it lacks also a neutral, or Bogomol’nyi saturated phase, where the (static Euclidean) stress–energy tensor would have vanished leading to noninteracting solitons. Thus

---

<sup>2</sup>Unlike here, in Refs.[3, 4], an explicit potential was not employed. This is because there, *only one* value,  $\omega = 0$ , was used so it was considered reasonable to treat the role of the corresponding potential in a putative capacity. This is justified since, as we have verified here too, the explicit use of a potential only affects the asymptotics of the chiral function  $f(r)$  and otherwise leads to no qualitative differences.

the unique phase in which the solitons are supported is of special interest, especially if it were attractive because then the switching on of  $\kappa$  would most likely not result in a crossover to a repulsive phase. We have verified that this is precisely what happens, as illustrated in Fig. 4 for the magnetic charge-2 soliton. An outstanding problem in this context is the calculation of the (attractive) interaction energy of two 1-monopoles as a function of their separation. This would demonstrate the existence of bound states definitively.

In addition to verifying that these models support mutually attracting like monopoles, we sought some indications as to whether there is the possibility of forming bound states of monopole charge greater than 2. (Apart from its intrinsic interest, the formation of very large monopole clumps may be relevant in cosmology.) To this end, axially symmetric solutions with monopole charges  $n = 2, 3, 4$ , for the  $\kappa = 0$ ,  $\kappa = 3$ , and the  $\kappa = 5$  models were constructed. It was seen that all these solitons remained in attractive phases. While it is expected that these axially symmetric solitons with  $n > 2$  are not the lowest energy solutions, the latter probably exhibiting (solid) Platonic symmetries [11, 12] as in the usual Skyrme model, it is nonetheless true that they give a reliable indication towards the existence of such bound states. To this end we list the binding energies against the dissociation of an axially symmetric charge- $n$  monopole into a charge- $n - 1$  and a charge-1 monopole in the last Table of Section 4. We see that this binding energy stays positive and does not change too much as  $n$  increases, at least for  $n \leq 4$ . Unfortunately the numerical process was not reliable much beyond  $n = 4$ .

While in the present work our primary aim has been the qualitative study of the solitons of the gauged Skyrme model characterised by  $\omega \neq 0$ , and the resulting property of the interaction of like monopoles in these theories, it may be in order to emphasise some physically attractive features of these models. These models combine some attractive features of (a) Higgs models, in this case the Georgi-Glashow model in that they support monopoles, and features of (b) Skyrme models, in this case the usual Skyrme model [1] in that the like-charged solitons are in an attractive phase. Indeed it appears that the attraction properties of these models are considerably more pronounced than those of the Skyrme model [1].

Apart from the practical consideration of the possibility of supporting large monopole clumps, there are two theoretical properties of the models that deserve mention. One is the physically desirable property of the symmetry breaking from  $SU(2)$  to  $U(1)$ , and the other one is the fact that the  $\kappa = 0$  model supports solitons with much the same qualitative properties as the generic models. The considerable advantage of this is that we avail of the Skyrme theoretic feature of mutually attracting solitons without having to pay the price of featuring a (quartic kinetic) Skyrme term in the Lagrangian, thus avoiding the attendant severe problems of quantisation.

**Acknowledgements:** We are indebted to B. Kleihaus for his collaboration at the initial stage of this investigation. This work was carried out in the framework of projects SC/96/602 and IC/00/021 of Enterprise-Ireland. We would like to thank the RRZN Hannover for computing time.

## References

- [1] T.H.R. Skyrme, Nucl. Phys., Proc. Roy. Soc. **A 260** (1961) 127; Nucl. Phys. **31** (1962) 556.
- [2] E. D'Hoker and E. Farhi, Nucl. Phys. **B 241** (1984) 109.
- [3] K. Arthur and D.H. Tchrakian, Phys. Lett. **B 352** (1995) 327.
- [4] Y. Brihaye and D.H. Tchrakian, Nonlinearity **11** (1998) 891.
- [5] B. Kleihaus, D.H. Tchrakian and F. Zimmerschied, J. Math. Phys. **41** (2000) 816.
- [6] V.B. Kopeliovich and B.E. Shtern, JETP Lett. **45** (1987) 203.
- [7] B. Kleihaus, D. O'Keeffe and D.H. Tchrakian, Nucl. Phys. **B 536** (1998) 381.
- [8] B. Julia and A. Zee, Phys. Rev. **D 11** (1975) 2227.
- [9] Y. Brihaye, B. Kleihaus and D.H. Tchrakian, J. Math. Phys. **40** (1999) 1136.
- [10] B. Kleihaus, J. Kunz and D.H. Tchrakian, Mod. Phys. Lett. **A 13** (1988) 2523.
- [11] E. Braaten, S. Townsend and L. Carson, Phys. Lett. **B 235** (1990) 147.
- [12] R. Battye, P. Sutcliffe, Phys. Rev. Lett. **79** (1997) 363.

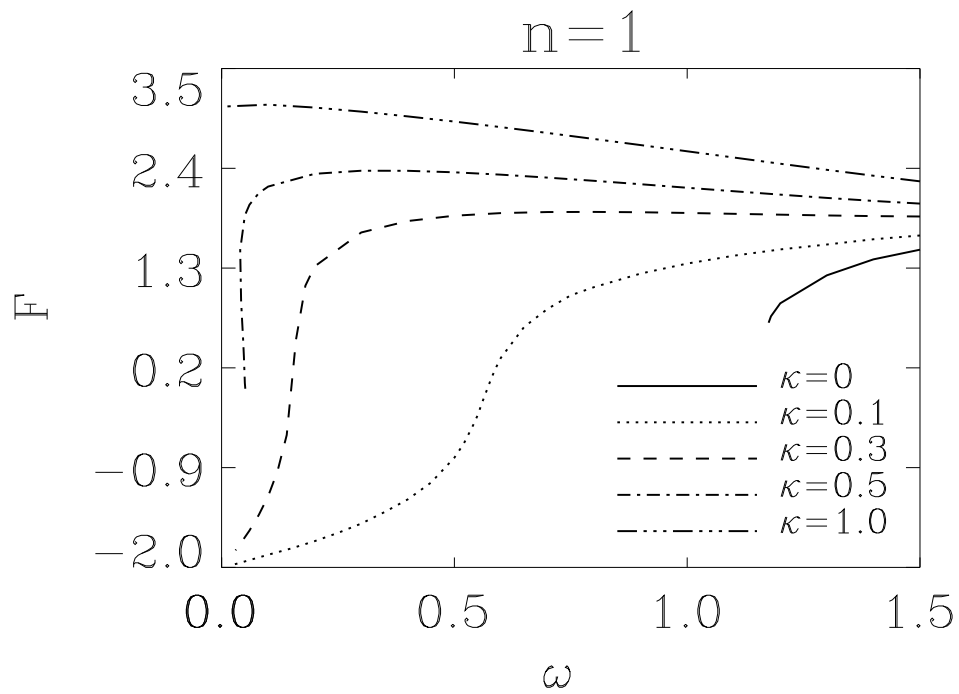


Figure 1: The quantity  $F$ , that determines the asymptotic behaviour of the skyrme field function  $f$  with  $f(x \gg 1) = \omega + F/x + o(1/x^2)$  is shown as a function of  $\omega$  for  $n = 1$  and different values of  $\kappa$ .

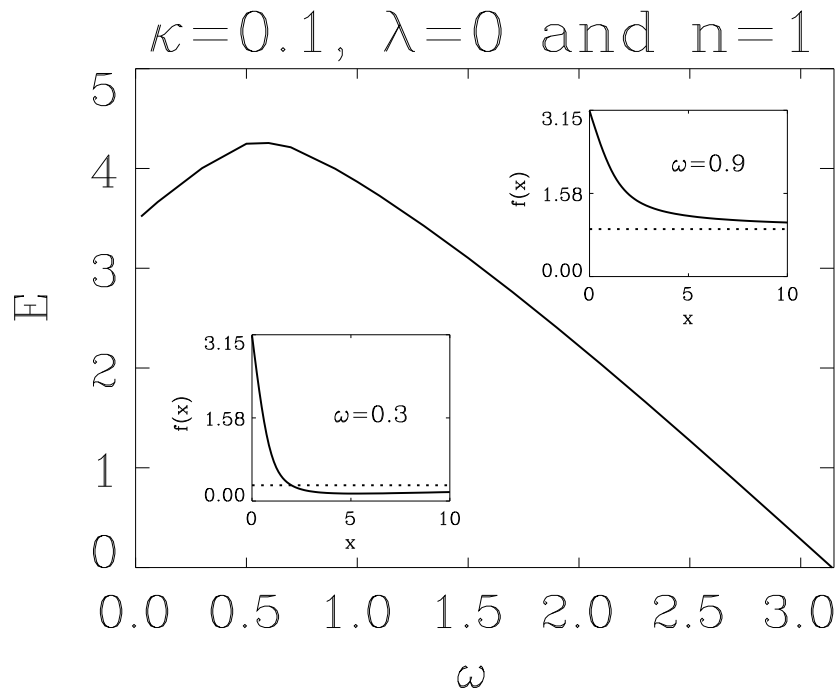


Figure 2: The energy  $E$  of the  $n = 1$  solution is shown as a function of  $\omega$  for  $\kappa = 0.1$  and  $\lambda = 0$ . The two insets show the skyrmion field function  $f(x)$  as function of the radial coordinate  $x$  for a)  $\omega = 0.3 < \omega_{max}$  and b)  $\omega = 0.9 > \omega_{max}$ .

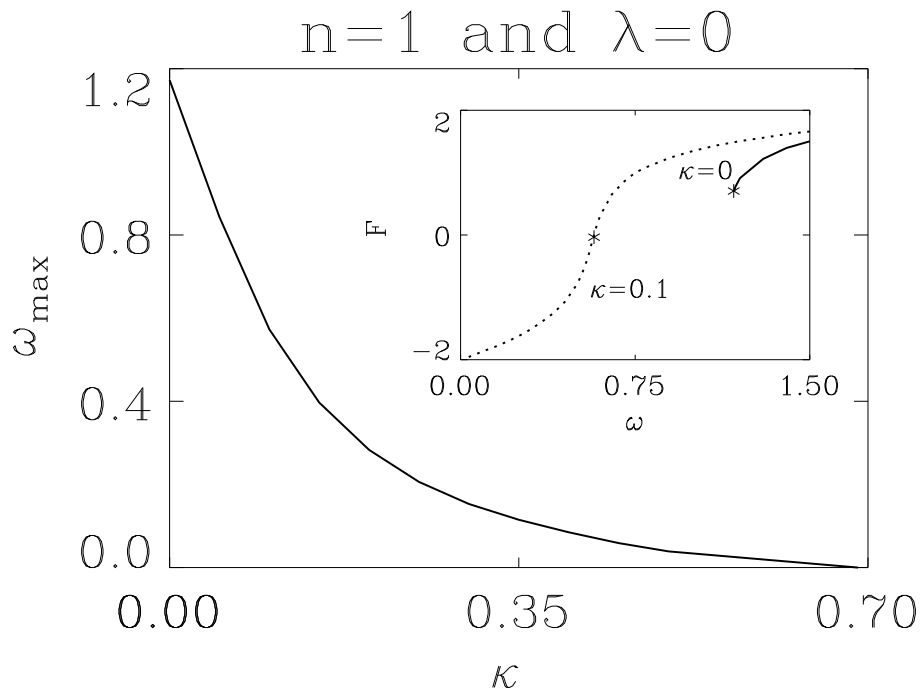


Figure 3:  $\omega_{max}$ , the value of  $\omega$  at which the energy has its maximum, is shown as function of  $\kappa$ . The inset shows the quantity  $F$  (see Fig.1) over  $\omega$  for  $\kappa = 0$  and 0.1. The asteriks mark  $\omega_{max}(\kappa)$ .

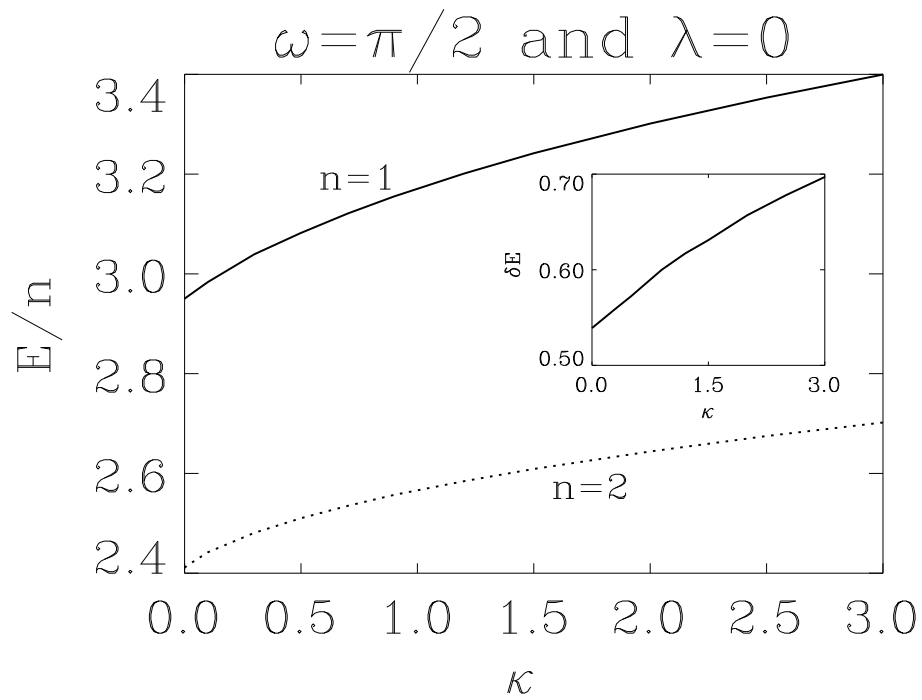


Figure 4: The energy per winding number  $E/n$  is shown as a function of  $\kappa$  for  $n = 1$  and  $n = 2$ ,  $\omega = \pi/2$  and  $\lambda = 0$ . The inset shows the difference of the energy per winding number  $\delta E = E(n = 1) - E(n = 2)/2$  between the  $n = 1$  and the  $n = 2$  solution.